



ELSEVIER

Physics Letters B 533 (2002) 43–59

PHYSICS LETTERS B

[www.elsevier.com/locate/npe](http://www.elsevier.com/locate/npe)

# Describing $F_2$ through a finite sum of gluon ladders

M.B. Gay Ducati<sup>a</sup>, K. Kontros<sup>b</sup>, A. Lengyel<sup>b</sup>, M.V.T. Machado<sup>a</sup><sup>a</sup> Instituto de Física, Universidade Federal do Rio Grande do Sul, Caixa Postal 15051, CEP 91501-970, Porto Alegre, RS, Brazil<sup>b</sup> Institute of Electron Physics, National Academy of Sciences of Ukraine, Universitetska 21, UA-88016 Uzhgorod, Ukraine

Received 20 February 2002; received in revised form 19 March 2002; accepted 21 March 2002

Editor: M. Cvetič

## Abstract

Electroproduction in deep inelastic scattering at HERA is studied in a model considering a finite sum of gluon ladders, associated with a truncation of the BFKL series. The approach contains the bare two gluon exchange and both one and two rungs contributions. The model is fitted to the data on the inclusive structure function  $F_2(x, Q^2)$  in the region  $x < 0.025$  and  $0.045 < Q^2 < 1500 \text{ GeV}^2$ , with a good agreement. Such a description for a large span in  $Q^2$  is obtained through a suitable modeling of the remaining non-perturbative background.

© 2002 Elsevier Science B.V. Open access under [CC BY license](https://creativecommons.org/licenses/by/4.0/).

## 1. Introduction

The high energy limit of the photon–proton scattering has been one of the main open questions concerning perturbative QCD and there is a great theoretical challenge in describing such process. The successful renormalization group approach summing the contributions of order  $(\alpha_s \ln Q^2)^n$ , namely, the DGLAP evolution equations [1], which has described systematically the deep inelastic data (gluon driven) starts to present slight deviations as the energies reached in the current experiments have increased [2]. Although its limitation has been theoretically determined [3], the DGLAP approach has enough flexibility to describe virtual photon initiated reactions on both low and high virtualities at small  $x$  [4]. Despite this fact, non-linear effects to the standard DGLAP formalism, associated with parton (mainly gluons) saturation and unitarity

corrections [5], are already known and their importance to describe the relevant observables at small  $x$  and estimate the future measurements is not negligible [6].

On the other hand, the high energy QCD calculation encoded in the leading logarithmic approximation (LLA) BFKL formalism [7] summing the contributions  $(\alpha_s \ln(1/x))^n$  is a powerful technique to perform predictions to the physical processes where a clear hard scale takes place, in which the approximation of fixed strong coupling (instead of running) in some external scale of the process is considered. This evolution equation provides the  $x$  evolution of the gluon density at small  $x$ . The main difficulty regarding this approach is the resulting total cross section for the BFKL pomeron exchange that violates the unitarity limit, stated by the Froissart limit  $\sigma_{\text{tot}} \leq \ln^2(s)$  [8] ( $\sqrt{s}$  is the center of mass energy), in hadronic collisions. It is a general believe that this bound is also required in  $\gamma^*p$  reactions. Recently, the next-to-leading (NLLA) BFKL calculation program has been accom-

---

E-mail address: [magnus@if.ufrgs.br](mailto:magnus@if.ufrgs.br) (M.V.T. Machado).

plished showing that the convergence of the series and its stability is far from clear at the moment [9]. Nevertheless, the unitarity problem has been addressed in Ref. [10], where the multiple LO BFKL pomeron exchanges dominate over the next order corrections and then the final scattering amplitude is unitarized. Such an approach gives rise to an evolution equation for the parton densities matching several statements of the saturation approaches mentioned above.

Recently, we have proposed a different phenomenological way to calculate the total cross sections in the hadronic sector [11], i.e., proton–(anti)proton collisions, and in deep inelastic scattering [12]. As a starting point, in Ref. [13] the reliability to describe the  $pp$  ( $p\bar{p}$ ) total cross sections through a QCD inspired calculation was shown to be successful. The main point is: at finite total energies, the LLA and NLLA summation implies that the amplitude is represented by a finite sum on terms, where the number of terms increases like  $\ln s$ , rather than by the solution of the BFKL integral equation. So one perform a truncation in the BFKL series and use it for a phenomenological description of the non-asymptotic energy data. The interest in to take the first terms in the complete series in the truncation is related to the fact that the energies reached by the present accelerators are not high enough to accommodate a big number of gluons in the ladder rungs that eventually hadronize. Corroborating this hypothesis, for example, the coefficient weighting the term  $\sim \ln^3 s$  turn out to be compatible with zero considering even the Tevatron data [13], in contrast with the expected from the complete resummation. This finding suggest that energies reached by the present accelerators are not yet asymptotic.

Moreover, in the present theoretical scenario the NLO corrections to the LO BFKL approach were accomplished, which lead to a decreasing of the hard pomeron intercept, issues about the running coupling constant and modifications in the correspondent anomalous dimension (for a short review, see [9]). Definitive answers concerning the NLO solution are now far from clear, imposing severe limits on the possible applicability of those results to the experimental situation (see, for example, [14]). Some remaining pathologies has been cured in the generalization of the high energy factorization formula in next-to-leading approximation by Ciafaloni and collaborators [15]. The improving procedure is the identification of the collinearly-

enhanced physical contributions as the most important agent of the instability of the BFKL hierarchy. Although of this reasonably determined theoretical status, a comparison of the underlying expressions with the deep inelastic data like in the case of LO BFKL was not performed yet. Indeed, currently the main focus is for processes with a predominantly hard scale, for instance  $\gamma^*\gamma^*$  or forward-jets, instead a two scale process like DIS. More specifically, in the full resummation of the BFKL series even at LLA there is not enough flexibility to perform modifications to consider the complete subleading contributions. A partial calculation of the subleading correction at the LO BFKL has been performed [16], taking into account dominant non-leading effects which come from the requirement that the virtuality of the exchanged gluons along the gluon ladder is controlled by their transverse momentum squared, restricting the available phase-space of the emitted gluons. Such a procedure can be used to perform predictions to observables to be measured.

Regarding the important question of take into account subleading contributions in a fixed order expansion of the BFKL approach, this issue was firstly addressed by Fiore et al. in the hadronic sector [13]. The coefficients of different powers of  $\ln(s)$  in the series refer to the dominant contribution, at asymptotic energies, for each perturbative order. However, when we perform a phenomenological description of data the subleading contributions are absorbed in the normalization constants for each ladder in the expansion or in the non-perturbative parameters of the model. This is the main factor of reliability lying in the data description of Refs. [13,17] and in our more detailed study for  $pp$  ( $p\bar{p}$ ) reactions in Ref. [11].

Motivated by the good result of the truncation in the hadronic case, we performed a more detailed calculation for those observables and extended the analysis to the non-forward region. Concerning high energy limit, the BFKL approach was a natural choice, since it takes into account a  $n$ -rung ladder contribution. To address a finite phase space for the gluon emission, disregarding the resummation and NLO effects intrinsic to the calculations, we consider that the possible exchanged ladders are built by a little number of gluon rungs. A non-asymptotic cross section is obtained considering only the one rung contribution ( $\sigma_{\text{tot}} \sim \ln s$ ), which is enough to describe the available data [11]. The non-zero momentum transfer calculation was per-

formed and the role played by a suitable choice of the proton impact factor was determined. Moreover, an useful parametrization for the elastic slope  $B_{\text{el}}(s)$  [11], consistent with the Regge phenomenology, was introduced allowing to describe with good agreement the differential cross section. The main features coming from that calculation are also corroborated by the phenomenological studies in Ref. [17].

Focusing on the deep-inelastic scattering, the similar motivation for the truncation of the perturbative series is the small phase space to allow an infinite gluon cascade in the final state. Some authors even advocate that the resummation technique in deep inelastic is not completely correct [18]. Indeed, in the available energies there is no room on pseudorapidity to enable a completely resummed  $n$ -rung ladder and studies have reported a strong convergence of the BFKL series considering few orders in the expansion (for example, in heavy vector meson production [18]). Furthermore, there is important evidence that the asymptotic solution to the BFKL equation is inappropriated in the most of the HERA range [18], and the expansion order by order allows to identify the onset of the region where the full BFKL series resummation is required.

In our previous work on this subject [12], we summed up two terms of the perturbative expansion and obtained the imaginary part of the DIS amplitude, hence the inclusive structure function  $F_2(x, Q^2)$ . Using the most recent HERA data on the  $F_2$ -logarithmic slope to determine the adjustable parameters at the small- $x$  region, we performed a broadly description of the structure function and its slope in the kinematical range of momentum fraction  $x < 10^{-2}$ . The resulting  $F_2$  and its gluon content turn out having a mild logarithmic growth as  $x$  diminishes in contrast with the steeper increasing from the usual DGLAP or BFKL dynamics, which we discuss a little more in the next section. It was also determined that the non-perturbative background is not negligible in all the kinematical region and should be better addressed. A remaining question in those previous works is the role played by the next order in the perturbative expansion and the modeling of the soft background, object of this work. To address the issues above, here one performs a more detailed study on the inclusive structure function considering the additional two rung contribution for the truncated series. With the introduction of this new term the virtual photon–proton cross section

reaches the behavior settled by the Froissart bound, i.e.,  $\sigma_{\text{tot}}^{\gamma^*p} \sim \ln^2(1/x)$ , however, keeping in mind that it is a result coming from a non-asymptotic series. Moreover, generally speaking, the BFKL pomeron is only a perturbative approximation to the true pomeron (valid at a limited kinematical range), of which the exact properties are unknown making it necessary to include some contribution of non-perturbative physics. We included the non-perturbative pomeron in two quite different forms, described latter on. As a result, the experimental data on the structure function  $F_2$  are successfully described in a broader region of  $(Q^2, x)$  variables and a more refined determination of the non-perturbative background is performed.

The final picture is quite similar to the two-pomeron one, where the hard and soft pomerons play an equally important role in data description.

This Letter is organized as follows. In the next section one introduces the main formulae and the most important features for the inclusive structure function, including the two rung contribution. In Section 3, an overall fit to the recent deep inelastic data is performed based on the present calculations and a suitable modeling for the non-perturbative background in two forms are introduced. As a byproduct, the resulting slopes are also shown. Finally, in the last section we draw our conclusions.

## 2. Finite sum of gluon ladders in deep inelastic scattering

Regarding the deep inelastic scattering reaction, the total cross section for the process  $\gamma^*p \rightarrow X$ , where  $X$  states for all possible final states, is obtained from Optical theorem through the imaginary part of the elastic  $\gamma^*p \rightarrow \gamma^*p$  amplitude. In the limit of very high energies the BFKL approach [7] is the most natural approach to treat such a process and is considered to compute the correspondent cross section [22]. As already discussed in the introduction, the main trouble with that framework are the unitarity violation coming from the LLA pomeron exchange and the known strong NLO corrections. In previous calculations we have proposed the truncation of the complete series in order to obtain an amplitude described by a finite sum of gluon ladders [12]. Below, one presents the main kinematical variables, the calculation of the amplitude

up to the second order in the perturbative expansion and the correspondent  $F_2(x, Q^2)$  expression.

Here, we are interested in the high energy region  $W^2 \gg Q^2$ , where  $W$  is the center of mass energy of the system virtual photon–proton and  $Q^2$  is the virtuality of the probe photon. Defining the momentum fraction, i.e., Bjorken variable, as  $x \approx \frac{Q^2}{Q^2+W^2}$ , the inequality above implies  $x \ll 1$ , setting the small- $x$  regime. The proton inclusive structure function, written in terms of the cross sections for the scattering of transverse or longitudinal polarized photons, reads as

$$F_2(x, Q^2) = \frac{Q^2}{4\pi^2\alpha_{em}} [\sigma_T(x, Q^2) + \sigma_L(x, Q^2)]. \quad (1)$$

In the asymptotic high energy limit, for photons with polarization  $\lambda$ , the cross section is given by the convolution of a perturbative kernel, which provides the dynamics of the process, with the corresponding impact factors of the interacting particles,

$$\sigma_\lambda(x, Q^2) = \frac{\mathcal{G}}{(2\pi)^4} \int \frac{d^2\mathbf{k}_1}{\mathbf{k}_1^2} \frac{d^2\mathbf{k}_2}{\mathbf{k}_2^2} \Phi_\lambda^{\gamma^*}(\mathbf{k}_1) \times F(x, \mathbf{k}_1, \mathbf{k}_2) \Phi_p(\mathbf{k}_2). \quad (2)$$

Clarifying the notation,  $\mathcal{G}$  is the color factor for the color singlet exchange and  $\mathbf{k}_1$  and  $\mathbf{k}_2$  are the transverse momenta of the exchanged reggeized gluons in the  $t$ -channel. The  $\Phi_\lambda^{\gamma^*}(\mathbf{k}_1)$  is the virtual photon impact factor (with  $\lambda = T, L$ ) and  $\Phi_p(\mathbf{k}_2)$  is the proton impact factor. The first one is well known in perturbation theory at leading order [22], while the latter is modeled since in the proton vertex there is no hard scale to allow pQCD calculations.

The kernel  $F(x, \mathbf{k}_1, \mathbf{k}_2)$  contains the dynamics of the process and has been systematically determined in perturbative QCD [9]. The main properties of the LO kernel are well known [7] and the results coming from the NLO calculations indicate that the perturbative pomeron can acquire very significant subleading corrections [9]. The most important feature of the LLA BFKL pomeron is the leading eigenvalue of the kernel, leading to a steep rise with decreasing  $x$ ,  $F(x) \sim x^{-\varepsilon}/\sqrt{\ln 1/x}$ , where  $\varepsilon = 4\bar{\alpha}_s \ln 2 \approx 0.5$ . Therefore, the inclusive structure function will present a similar growth at low  $x$ . Hence, the resulting amplitude and consequently the total cross section or structure function, at first glance, overestimates the growing of the observable currently measured.

We proposed an alternative phenomenological way to calculate the observables at current energies, showing that a reliable description of both proton–(anti)proton and virtual photon–proton collisions is obtained considering the truncation up to two orders in the perturbative expansion [11,12]. In the accelerators domain the asymptotic regime is not reached and there is no room in rapidity to enable an infinite  $n$ -gluon cascade, represented diagrammatically by the BFKL ladder. Moreover, a steep convergence of the LO BFKL series in few orders in the perturbative expansion has been already reported [18] and phenomenological studies indicate that such a procedure is reasonable at least in proton–proton collision [13,17]. In order to perform the calculations, it should be taken into account the convolution between the photon and proton impact factors and the corresponding gluon ladder exchanges in each order. The Born contribution comes from the bare two gluon exchange and in the leading order the amplitude is imaginary at high energies and written for  $t = 0$  as

$$\mathcal{A}^{\text{Born}}(W, t = 0) = \frac{2\alpha_s W^2}{\pi^2} \sum_f e_f^2 \times \int \frac{d^2\mathbf{k}_1}{\mathbf{k}_1^4} \Phi_\perp^{\gamma^*}(\mathbf{k}_1) \Phi_p(\mathbf{k}_1). \quad (3)$$

The next order contribution is obtained from the graphs considering the one-rung gluon ladder and has the following expression in LLA

$$\begin{aligned} \mathcal{A}^{\text{one-rung}}(W, t = 0) &= \frac{6\alpha_s^2 W^2}{8\pi^4} \sum_f e_f^2 \ln(W^2/W_0^2) \\ &\times \int \frac{d^2\mathbf{k}_1}{\mathbf{k}_1^4} \frac{d^2\mathbf{k}_2}{\mathbf{k}_2^4} \Phi_\perp^{\gamma^*}(\mathbf{k}_1) K(\mathbf{k}_1, \mathbf{k}_2) \Phi_p(\mathbf{k}_2). \end{aligned}$$

The  $\alpha_s$  is the strong coupling constant, considered fixed since we are in the framework of the LO BFKL approach. As a remark, the running of the coupling constant contributes significantly for the NLO BFKL, since it is determined by subleading one-loop corrections, for example the self-energy and vertex-correction diagrams [9]. The typical energy of the process is denoted by  $W_0$ , which scales the logarithm of energy and takes an arbitrary value in LLA.

The perturbative kernel  $K(\mathbf{k}_1, \mathbf{k}_2)$  can be calculated order by order in the perturbative expansion and is encoded by the BFKL kernel if one considers the LLA resummation. In the present case,  $t = 0$  and it describes the gluon ladder evolution in the LLA of  $\ln(s)$  as already discussed above. The pomeron is attached to the off-shell incoming photon through the quark loop diagrams, where the reggeized gluons are attached to the same and to different quarks in the loop [12]. Since the transverse contribution dominates over the longitudinal one, hereafter  $\Phi_{\perp}^{\gamma^*}$  is the virtual photon impact factor averaged over the transverse polarizations [23],

$$\Phi_{\perp}^{\gamma^*}(\mathbf{k}_1) = \frac{1}{2} \int_0^1 \frac{d\tau}{2\pi} \int_0^1 \frac{d\rho}{2\pi} \frac{\mathbf{k}_1^2 (1 - 2\tau\tau')(1 - 2\rho\rho')}{\mathbf{k}_1^2 \rho\rho' + Q^2 \rho\tau\tau'}, \quad (4)$$

where  $\rho, \tau$  are the Sudakov variables associated to the momenta in the photon vertex and the notation  $\tau' = (1 - \tau)$  and  $\rho' = (1 - \rho)$  is used, Ref. [22].

A well-known fact is that we are unable to compute the proton impact factor  $\Phi_p(\mathbf{k}_2)$  using perturbation theory since it is determined by the large-scale nucleon dynamics. However, gauge invariance requires that  $\Phi_p(\mathbf{k}_2 \rightarrow 0) \rightarrow 0$  and then the proton impact factor can be modeled as a phenomenological input obeying that limit and takes a simple form

$$\Phi_p(\mathbf{k}_2) = \mathcal{N}_p \frac{\mathbf{k}_2}{\mathbf{k}_2 + \mu^2}, \quad (5)$$

where  $\mathcal{N}_p$  is the unknown normalization of the proton impact factor and  $\mu^2$  is a scale which is typical of the non-perturbative dynamics. Furthermore, these non-perturbative parameters can absorb possible sub-leading contribution in each order of the perturbative expansion [12].

Considering the electroproduction process, summing the two first orders in perturbation theory we can write the expression for the inclusive structure function, whose contributions have been already discussed (Section V of Ref. [23])

$$F_2(x, Q^2) = \frac{8}{3} \frac{\alpha_s^2}{\pi^2} \sum_f e_f^2 \mathcal{N}_p \left( F_2^{\text{Born}}(Q^2, \mu^2) + \frac{3\alpha_s}{\pi} \ln\left(\frac{x_0}{x}\right) F_2^{(1)}(Q^2, \mu^2) \right), \quad (6)$$

where the functions  $F_2^{\text{Born}}(Q^2, \mu^2)$  and  $F_2^{(1)}(Q^2, \mu^2)$  (I meaning one-rung contribution) given by

$$F_2^{\text{Born}}(Q^2, \mu^2) = \frac{1}{2} \ln^2\left(\frac{Q^2}{\mu^2}\right) + \frac{7}{6} \ln\left(\frac{Q^2}{\mu^2}\right) + \frac{77}{18},$$

$$F_2^{(1)}(Q^2, \mu^2) = \frac{1}{6} \ln^3\left(\frac{Q^2}{\mu^2}\right) + \frac{7}{12} \ln^2\left(\frac{Q^2}{\mu^2}\right) + \frac{77}{18} \ln\left(\frac{Q^2}{\mu^2}\right) + \frac{131}{27} + 2\zeta(3), \quad (7)$$

where  $x_0$  gives the scale to define the logarithms on energy for the LLA BFKL approach (is arbitrary and enters as an additional parameter) and  $\zeta(3) = \sum_r (1/r^3) \approx 1.202$  is the Riemann  $\zeta$ -function.

Connecting the present result to the Regge phenomenology, the truncation of the perturbative series reproduces the main characteristics coming from the Regge-dipole pomeron model. In the dipole pomeron the structure function is  $F_2(x, Q^2) \sim R(Q^2) \ln(1/x)$ , whose behavior corresponds to the contribution of a double  $j$ -pole to the partial amplitude of  $\gamma^* p \rightarrow \gamma^* p$ , where  $R(Q^2)$  is the pomeron residue function. Moreover, the dipole pomeron trajectory has unit intercept,  $\alpha_{\mathbb{P}}(0) = 1$ , and has been used in several phenomenological fits to hadronic sector and HERA data [24]. While in the dipole pomeron picture the residue is factorized from the energy behavior in the amplitude, the  $Q^2$ -dependence is calculated order by order in perturbation theory in our case.

In Ref. [12], we choose to determine the parameters of the model ( $\mu, x_0$  and  $\mathcal{N}_p$ ) from a smaller data set, meaning the latest HERA measurements on the  $Q^2$ -logarithmic derivative reported by the H1 [19] and ZEUS Collaboration (preliminary). The reasons for that are the consistent and precise measurements of the slope and the additional fact that using the  $Q^2$  derivative we avoid contributions from the non-perturbative background depending weakly on  $Q^2$ . The obtained values were consistent with the naive estimates, namely  $\mu^2$  would be in the non-perturbative domain ( $\mu \approx \Lambda_{\text{QCD}}$ ) in both data sets and  $x_0$  has a value consistent with the Regge limit. The fitted expression to the slope described the data with good agreement, producing effectively the same linear behavior in  $\ln Q^2$  considered by the H1 Collaboration fitting analyzes. Considering the  $x$  dependence of the slope, a gluon distribution softer than those coming from the usual approaches,  $xG(x, Q^2) \sim x^{-\lambda}$  [1,7] is

obtained towards small  $x$ . The growth of the structure function shown large deviations from the steep increasing present at both LO BFKL series and DGLAP approach, where  $F_2 \sim x^{-\lambda}$ . The non-perturbative contribution (from the soft dynamics), mainly at low  $Q^2$  virtualities, was found not negligible. One estimated that those effects imply correction of  $\approx 20\%$  in the overall normalization.

In the next section we address the effects of introducing the next order in the perturbative expansion and a more refined parametrization for the non-perturbative background. In order to do so, we need to calculate the two-rung contribution in the ladders summation. Following the calculations [12,23], it results

$$\begin{aligned}
 F_2^{(\text{II})}(x, Q^2) &= \frac{8}{3} \frac{\alpha_s^2}{\pi^2} \sum_f e_f^2 \mathcal{N}_p \left[ \frac{1}{2} \left( \frac{3\alpha_s}{\pi} \ln \frac{x_0}{x} \right)^2 \right. \\
 &\times \left( \frac{1}{24} \ln^4 \frac{Q^2}{\mu^2} + \frac{7}{36} \ln^3 \frac{Q^2}{\mu^2} + \frac{77}{36} \ln^2 \frac{Q^2}{\mu^2} \right. \\
 &\quad \left. + \left( \frac{131}{27} + 4\zeta(3) \right) \ln \frac{Q^2}{\mu^2} \right. \\
 &\quad \left. \left. + \frac{1396}{81} - \frac{\pi^4}{15} + \frac{14}{3} \zeta(3) \right) \right], \quad (8)
 \end{aligned}$$

where the notation is the same one of the expressions above and such a contribution should be added to the previous results in order to perform a fit to the HERA data. Our final fitting expression is then given by

$$\begin{aligned}
 F_2(x, Q^2) &= F_2^{\text{Born}} + F_2^{(\text{I})}[\text{one-rung}] \\
 &\quad + F_2^{(\text{II})}[\text{two-rung}] \\
 &\quad + F_2^{\text{soft}}[\text{Background}]. \quad (9)
 \end{aligned}$$

Some remarks about the results derived from the truncation of the perturbative series are in order. An important issue emerging is the role of the subleading contributions at a fixed order expansion of the BFKL approach, firstly addressed by Fiore et al. in the hadronic sector [13]. The coefficients of different powers of  $\ln(s)$  in the series refer to the dominant contribution, at asymptotic energies, for each perturbative order. However, performing a phenomenological description of data the subleading contributions are absorbed into the normalization constants for each ladder in the expansion, or in the non-perturbative parameters of the model. This can shed light about the

strength of those contributions in the description of the observables. For instance, in Ref. [13] it was found that already at the Tevatron energy range, the coefficient weighting the term  $\ln^3(1/x)$  is approximately equal to zero in contrast with the expectations from the perturbative coefficient calculated in the complete series. This is the main feature of reliability in the data description of Refs. [13,17] and in our more detailed study for  $pp$  ( $p\bar{p}$ ) reactions in Ref. [12].

Concerning the gluon content of  $F_2$ , in general grounds the truncated series provides a mild logarithmic growth instead a steep one from DGLAP or LO BFKL resummations. In order to illustrate the result coming from adding rungs in the ladder, that is summing new terms in the truncation, we can make use of the effective exponent of  $F_2$ . One can parametrize the increasing of the structure function (and the gluon content at small- $x$ ) in the simple form  $F_2(x, Q^2) \simeq x G(x, Q^2) \approx f(Q^2) x^{-\lambda_{\text{eff}}}$ , where we can calculate the exponent as  $\lambda_{\text{eff}} = d \ln F_2 / d \ln(1/x)$ .

The Born two-gluon approximation to  $F_2$ , i.e., first term in Eq. (6), provides a constant contribution on  $\ln(1/x)$  and, therefore, it gives  $\lambda_{\text{eff}} = 0$ . Of course, this result is rule out by the experimental measurements. When one introduces the one-rung piece, turn out  $F_2 = f_0(Q^2) + f_1(Q^2) \ln(1/x)$ , where  $f_0$  and  $f_1$  are the  $Q^2$ -dependent (logarithmic) factors appearing in Eq. (6). The resulting effective exponent is thus  $\lambda_{\text{eff}} = [f_0/f_1 + \ln(1/x)]^{-1}$ . If we consider the approximation  $f_0/f_1 \ll 1$  at fixed  $Q^2$ , which it seems reasonable from inspection of Eqs. (7), (8), one estimates that the effective intercept takes values between  $\lambda_{\text{eff}} \simeq 0.2$  at  $x = 10^{-2}$  and decreasing to  $\lambda_{\text{eff}} \simeq 0.1$  for  $x \sim 10^{-5}$ . This growth is softer than the typical DGLAP result  $\lambda_{\text{eff}} \simeq 0.3$ . Concerning the addition of the two-rung piece, the result is less simple; however, if we consider the limit case where  $f_2(Q^2) \gg f_1(Q^2), f_0(Q^2)$ , one obtains  $\lambda_{\text{eff}} \approx 2/\ln(1/x)$ . Then, the effective exponent would take values 0.4 at  $x = 10^{-2}$  and saturating at 0.2 around  $x \sim 10^{-5}$ : values quite similar to the mean value from DGLAP expectations. The results estimated above have implications for instance on diffraction. The  $x_{\mathbb{P}}$  dependence of the diffractive structure function,  $F_2^D$ , depends directly on the unintegrated gluon distribution  $\mathcal{F}(x_{\mathbb{P}}, k_T) = k_T^2 \partial_x G(x, k_T^2) / \partial k_T^2$  and then one expects a mild logarithmic increasing and a non-trivial (logarithmic)  $k_T$  dependence.

Now, having the expression for the inclusive structure function at hand, in the next section we compare it with the HERA experimental results, determining the adjustable parameters and the range of validity for this model.

### 3. Fits to the HERA data: choice of background and discussion of the results

In order to compare the expression obtained to the structure function  $F_2(x, Q^2)$ , Eq. (9), with the experiment, we choose to use the updated HERA data set starting from the smallest available  $Q^2$  for small- $x$  region  $x \approx 10^{-2}$ . The BFKL pomeron as well as its truncation should be valid in a specific kinematical interval, for instance the full series [25] can accommodate data ranging from  $1 \leq Q^2 \leq 150 \text{ GeV}^2$  in a good confidence level. For this purpose we need to include a soft background, accounting for the non-perturbative content and providing a smooth transition to  $Q^2 = 0$ . Notice that an extrapolation to the photoproduction region is still lacking in the present analysis, although we have a definite expression for that [12]. Thus, here we consider the electroproduction case and the low virtualities range will be driven by the non-perturbative background, modeled through a soft pomeron. There exists numerous possibilities from novel [27–29] to previous [30] models, which give significant contribution in the data description for  $Q^2 \leq 10 \text{ GeV}^2$ . In our case, we use the model with the most economical number of parameters and for this purpose we have first selected the latest version [31] of the CKMT model [30]:

$$F_2^{\text{soft}}(x, Q^2) = A \left( \frac{x_0}{x} \right)^{\Delta(Q^2)} \left( \frac{Q^2}{Q^2 + a} \right)^{\Delta(Q^2)+1}, \quad (10)$$

where the expression for  $\Delta(Q^2)$  has the following form:

$$\Delta(Q^2) = \Delta_0 \left( 1 + \frac{Q^2 \Delta_1}{\Delta_2 + Q^2} \right). \quad (11)$$

where  $\Delta(Q^2)$  is the pomeron intercept and the remaining parameters are defined in [30]. Such a model considers a soft pomeron which is a single pole in the complex angular momentum plane having a  $Q^2$ -dependent intercept. Although formally it is not a pure

Regge approach, it describes the low virtuality region with very good agreement [30] with a limited number of adjustable parameters. The dependence on  $Q^2$  of the structure function comes from the pomeron residue and in general is modeled since there is little theoretical knowledge, namely, vertex functions and couplings at the amplitudes. The gauge invariance only requires that it should vanish as  $Q^2 \rightarrow 0$ . Particularly, a model-independent way is more preferable, for instance, as performed by [27], where the residue function is extracted from data and then fitted with a suitable adjusting function.

Another possibility is to select a pomeron for the background which has an intercept equal to 1 and has the form of a non-perturbative truncated  $\log(Q^2/x)$  series (soft multipole pomeron) [28,29], with the form

$$F_2^{\text{soft}}(x, Q^2) = Q^2 \left[ a \left( \frac{d}{Q^2 + d} \right)^\alpha + b \ln \left( \frac{Q^2}{x} \right) \left( \frac{d}{Q^2 + d} \right)^\beta + c \ln^2 \left( \frac{Q^2}{x} \right) \left( \frac{d}{Q^2 + d} \right)^\gamma \right], \quad (12)$$

where this choice has a larger number of parameters than the previous background and we naively expect a better accommodation to the data. To proceed, we used two models for the background to fit the structure function  $F_2$ . The finite sum of gluon ladders is encoded in the Eqs. (6) and (8), while the soft pomeron is given by Eqs. (10) and (12). In both cases we have applied the factor  $(1-x)^7$  to provide the behavior of  $F_2$  at large- $x$  region and being the same for both soft and hard pomeron, extending the applicability of the models to the  $x \rightarrow 1$  region. From the dimensional-counting rules these threshold correction factors are given by  $(1-x)^{2n-1}$ , where  $n$  is the spectators number (for the pomeron it is equal 4). Thus, our considerations are consistent with this fact and should provide a good description even at large  $x$ .

For the fitting procedure we consider the data set containing all available HERA data for the proton structure function  $F_2$  [19,32,33,35–37,39,40]. Notice that the most recent measurements in H1 and ZEUS are more accurate (stat. error  $\approx 1\%$ ) than the previous ones, providing stringest constraints to the parameters. For the fit we have used 496 experimental points for  $x \leq 0.025$  and  $0.045 \leq Q^2 \leq 1500 \text{ GeV}^2$ . We selected

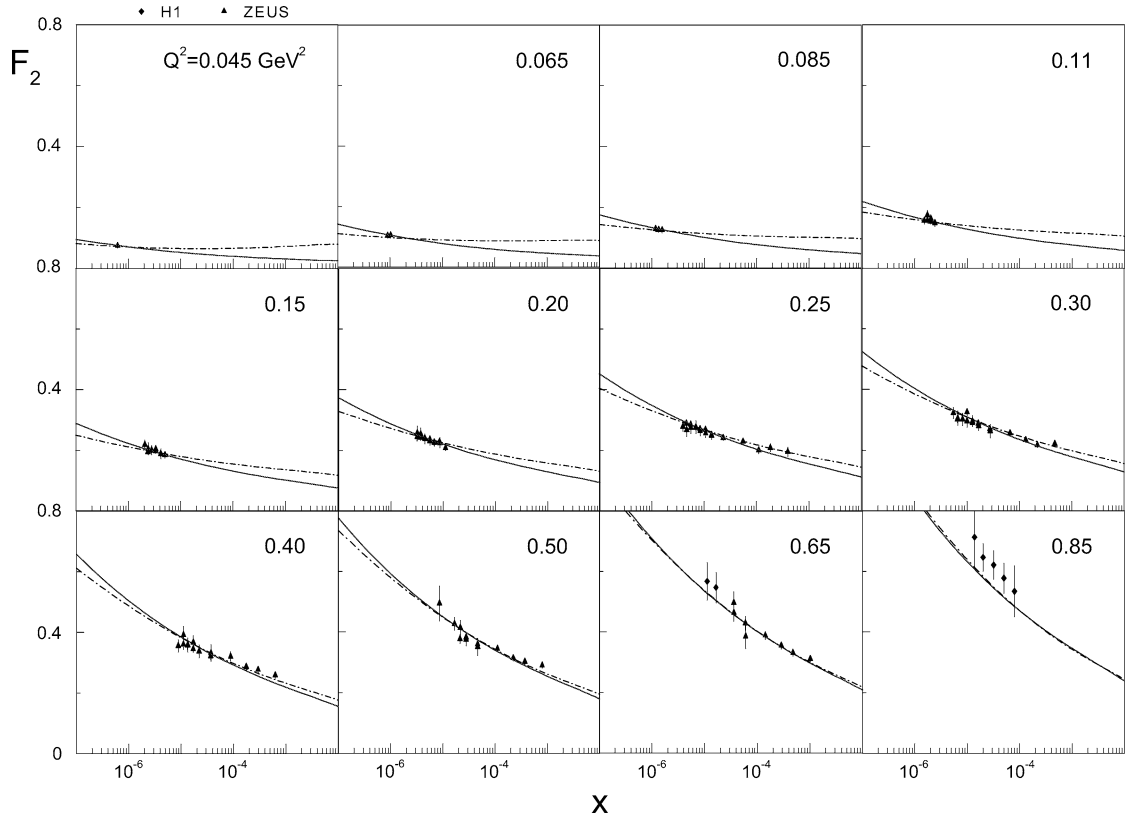


Fig. 1. The inclusive structure function at very small  $Q^2$  virtualities. The solid line corresponds to the model with the first background [Eqs. (10), (11)], while the dash-dotted line to the model with the second background [Eq. (12)].

the overall normalization factor as a free parameter for the hard pomeron contribution, Eq. (6), defined as

$$\mathcal{N} = \frac{8}{3} \frac{\alpha_s^2}{\pi^2} \sum_f e_f^2 \mathcal{N}_p,$$

considering four active flavours. In Figs. 1–3 we show the resulting fits considering the two distinct backgrounds. The best fit parameters of the model are shown in Tables 1, 2.

Before to proceed, we discuss how the results presented here compare with the previous ones using only two terms of the perturbative expansion and how the play ruled by the background is affected by adding a new term in the expansion. Considering only the finite sum of gluon ladders (hard pomeron) one obtains the following: using either the one rung ladder [Eq. (6)] as well as the two-rung contribution [Eqs. (6), (8)], the model provides the same  $\chi^2/\text{dof} = 1.6$  in the interval  $1.2 \leq Q^2 \leq 150 \text{ GeV}^2$ , whereas

the fit is degraded for a larger interval of virtualities (i.e.,  $\chi^2/\text{dof} \approx 2.5$  for  $1.2 \leq Q^2 \leq 800 \text{ GeV}^2$ ). These results are in agreement with the analysis [25] (limited to a specific H1 data set [38]), corroborating that the BFKL-like models accommodate data at virtualities up to  $\approx 150 \text{ GeV}^2$  [26]. This kinematical limit corresponds to the region where DGLAP resummation start to be important, that is the  $[\alpha_s \ln(Q^2/Q_0^2)]^n$  terms would dominate the  $\alpha_s \ln(1/x)^n$  contributions. The resulting  $\chi^2/\text{dof} = 1.6$  is still formally large in comparison with more phenomenological approaches, however, it can be justified if we note the little number of parameters considered (3 adjustable constants) and desconsidered the effects of large  $x$ . The main point is that the addition of a new term does not improve strongly the description of data. This fact is supported by the finding that the coefficient weighting the term  $\ln^2(1/x)$  in the expansion is significantly small in comparison with the  $\ln(1/x)$  term [13].



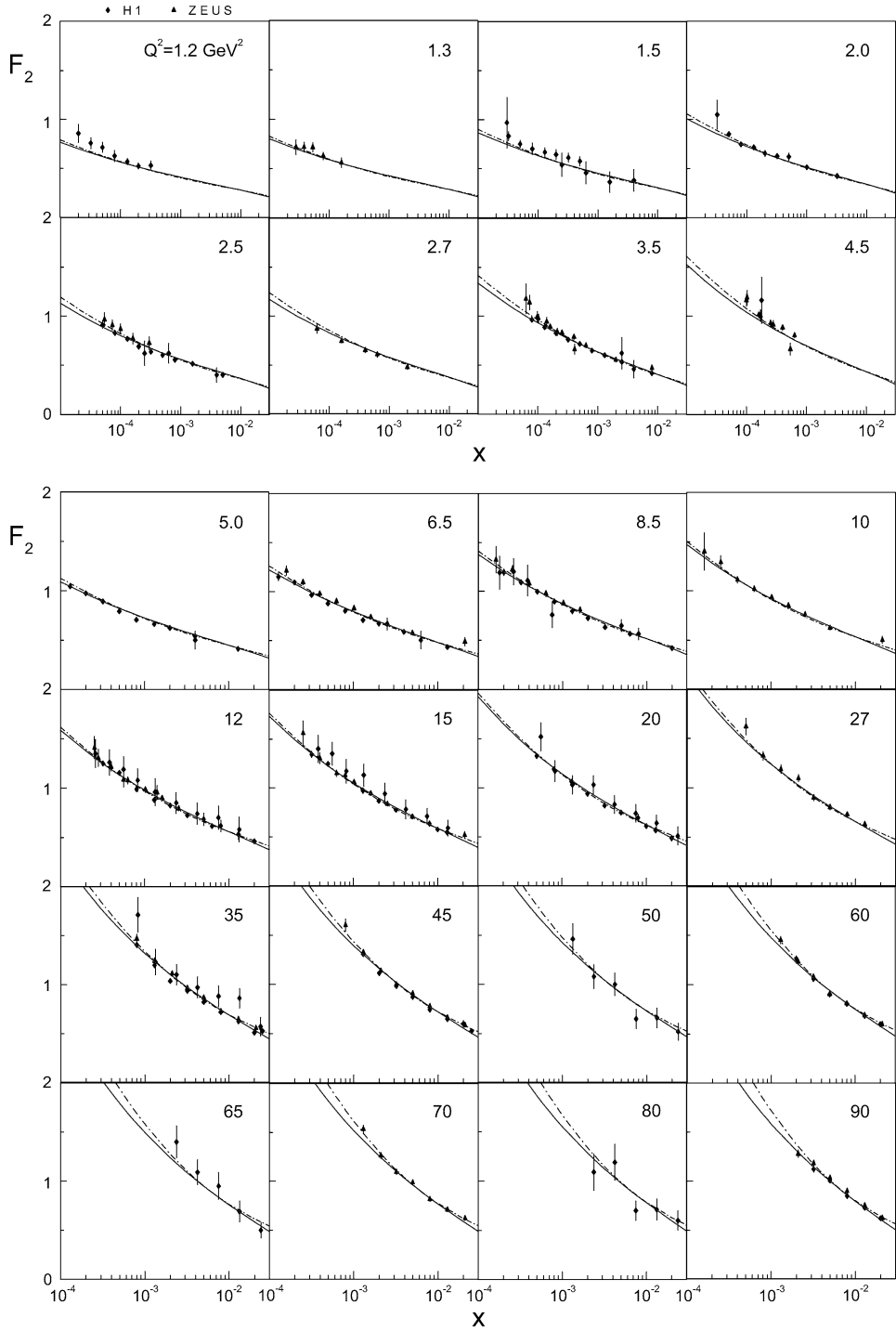


Fig. 2. The inclusive structure function at small and medium  $Q^2$  virtualities. Same notation of the previous plot.

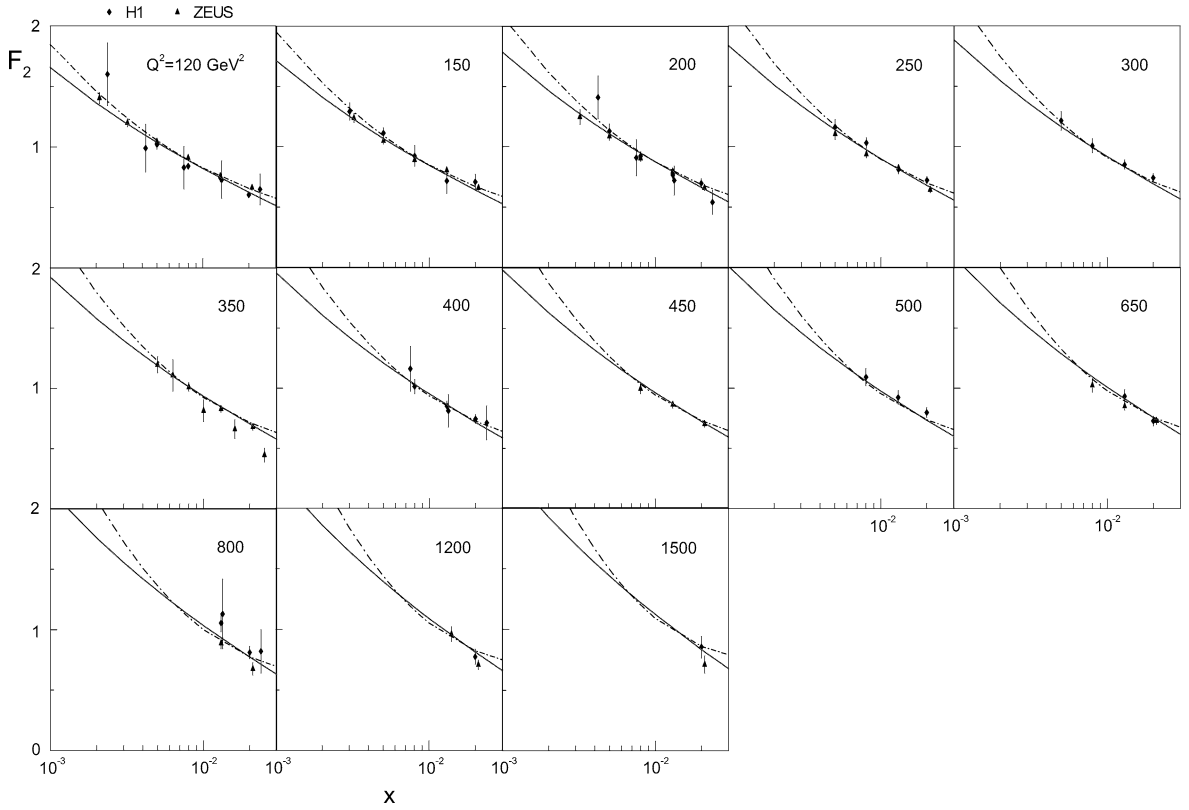


Fig. 3. The inclusive structure function at large  $Q^2$  virtualities. Same notation of the previous plots.

Table 1

Parameters of the model with the first background, Eq. (9), obtained from the fit

$\mathcal{N}$	$\mu^2$	$x_0$	$\alpha_s$	$A$	$a$	$\Delta$	$\Delta_1$	$\Delta_2$	$\chi^2$
0.00312	1.39	0.251	0.2 (fixed)	0.279	0.579	0.108	1.65	9.68	1.14

Table 2

Parameters of the model with the second background, Eq. (11), obtained from the fit

$\mathcal{N}$	$\mu^2$	$x_0$	$\alpha_s$	$a$	$b$	$c$	$\alpha$	$\beta$	$\gamma$	$d$	$\chi^2$
0.0191	0.593	0.148	0.242	0.506	-0.426	-0.0495	0.491	1.69	0.727	0.130	0.94

Concerning the role played by the background, the procedure used in the previous work [12] was somewhat different. We choose the slope data for fitting the parameters of the model for two reasons: (a) they are quite precise and are determined from the updated measurements of  $F_2$ ; (b) considering a derivative on  $Q^2$  we are avoiding the contributions from the non-perturbative background (depending weakly on  $Q^2$ ), which should be added to the final  $F_2$  expression.

There, we have multiplied the resulting  $F_2$  by a factor 1.2, in order to roughly simulate the background effects. Of course, this is only a naive estimation and leads to a worse description of data. However, the main point is that the background is important in data description over all the kinematical range and would be of order  $\approx 20\%$ . Here, we have modeled carefully the soft background based on Regge phenomenology for the pomeron. From the discussion about the resulting

effective exponent in the previous section, we naively expect that the background in the one-rung case would have a larger effect in mimic the measured  $\lambda_{\text{eff}}$  than in the two-rung case. Although we are not able to produce a reasonable comparison with the previous work due to the different procedure considered, the definitive finding is that the background is active in the full kinematical interval, instead of being important only in a specific range, and account for a non-negligible contribution to  $F_2$ .

Returning to the present analysis, the final result considering the additional soft background, is in agreement with data in a good confidence level for a large span of  $Q^2$ . The  $\chi^2$  values obtained select the logarithm-type as the better background. The negative value for the  $c$  constant is a non-favoured choice despite the better  $\chi^2/\text{dof}$ . Instead, if we consider only a  $\sim \log(Q^2/x)$  or  $\sim \log^2(Q^2/x)$  parametrization one gets a smaller number of parameters, however, the  $\chi^2/\text{dof}$  value becomes similar to the CKMT-type.

In Fig. 1 are shown the results for the low  $Q^2$  data, expected to be dominated by the soft pomeron background. Both choices for the soft pomeron seem to describe these data bins quite well, however, the CKMT-type one provides a steeper increasing with  $x$  than the log-type up to  $\approx 0.25 \text{ GeV}^2$ , which comes directly from the respective intercept for each background; above that virtuality both have the same behavior on Bjorken  $x$ .

In Figs. 2 and 3 one verifies that the description is independent of the specific choice for the soft pomeron, as expected, since in that kinematical region the finite sum of ladders dominates. At higher  $Q^2$  the description deviates following the different backgrounds: at  $Q^2 \approx 90 \text{ GeV}^2$  and increasing as virtualities get larger. However, the deviation is present in a kinematical region where no data is measured and does not allow an unambiguous conclusion. In general grounds, as it is seen from the figures and tables the model of finite sum of ladders with the logarithmic-type background describes better the entire data set and probably it would be even better for a wider interval of  $x$  and  $Q^2$ , but the CKMT-type contribution is phenomenologically preferred due to the smaller set of parameters considered.

Comparing the present analysis with the available Regge phenomenology, we have a description similar to the two-pomeron approach [27]: the hard pomeron

in our case is given by the finite sum of gluon ladders up to the two-rung contribution and the  $Q^2$ -dependence is completely determined from the perturbative expansion, truncated at order  $\alpha_s^4$ . An extrapolation to the photoproduction region is still lacking, which would be obtained once the impact factor of the photon is provided at  $Q^2 = 0$  and possible singularities are regulated. The hard pomeron couples to each quarks flavour with the same coupling, i.e., it is flavour-blind. In a similar way as [27], we naively expect roughly to describe the charm content  $F_2^{c\bar{c}}$  taking 2/5 of the hard-pomeron contribution (the fraction means  $e_c^2/(e_u^2 + e_d^2 + e_s^2)$ ). We verify that the backgrounds play a significant role not only at small  $Q^2$ , but in the whole interval considered, while the pieces separately give good results just for a relatively narrow- $x$  region. Undoubtedly, this hybrid approach is good for all  $x$  and  $Q^2$  if we use a proper behavior of  $F_2$  for large  $x$ , i.e., the use of an additional non-singlet term.

The model is still comparable with other Regge models, for instance, considering the very nice comparative phenomenological analysis of Ref. [29]. There, the two pomeron model, the soft dipole pomeron, a modified two pomeron model and a generalized logarithmic pomeron are analyzed in a large span of  $Q^2$  (including photoproduction). At small  $x$ , our data description is in agreement with them, having a similar  $\chi^2/\text{dof}$  (slightly larger for the CKMT background) and with a similar number of free-parameters (even smaller, for instance using CKMT background). The same conclusions are valid concerning the logarithmic fitting of  $F_2$  taken into account in Ref. [28] and in the analysis of Ref. [21]. The main advantage of the present approach is that the dependence on  $Q^2$  of the hard pomeron is completely determined from pQCD, in contrast with a model-dependent parametrization of the residue pomeron function in the Regge case.

Considering the QCD fit using the full BFKL series [25], our results without a background presents a slightly larger  $\chi^2/\text{dof}$  in a same fitting region ( $1.5 \leq Q^2 \leq 150 \text{ GeV}^2$ ). However, the good data description coming from [25] is obtained to the cost of a quite low value of the coupling constant (leading a lower intercept for the BFKL pomeron), maybe it mimics NLO corrections to the pomeron intercept. In our case, we have fixed the coupling constant in the reasonable value  $\alpha_s = 0.2$ , consistent with the virtualities, where

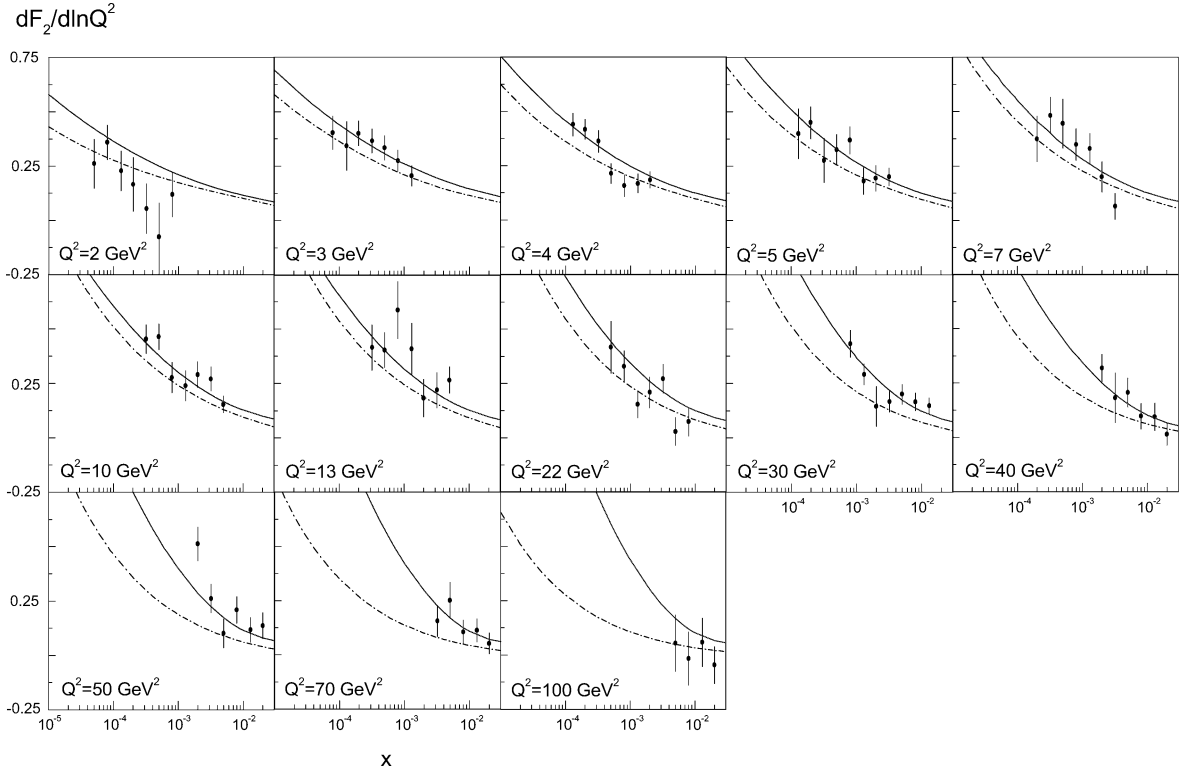


Fig. 4. The result for the  $B_Q$  slope plotted as a function of  $x$  for fixed  $Q^2$  virtualities compared with the latest H1 data [19]. The solid line corresponds to model with the first background [Eq. (9)], while the dash-dotted line to the model with the second background [Eq. (11)].

the fit is performed, and have noticed that the effect of left it free is almost negligible, for instance when we consider the logarithmic background.

In order to perform a detailed comparison between the results above we calculated the slopes of the proton structure function, which are presented in the next section.

#### 4. The logarithmic derivatives

The slopes of the proton structure function give valuable information concerning the behavior of the gluon distribution and the effective pomeron intercept. A considerably broad region of DIS kinematical region in the upcoming accelerator, i.e., THERA, will effectively enables to probe the saturation phenomenon and other asymptotic properties, which can be more explicit in derivative quantities directly dependent on the gluon content of the proton. For this

study it is most convenient to consider the logarithmic slopes, defined as follows:

$$B_Q(x, Q^2) = \frac{\partial F_2(x, Q^2)}{\partial \ln Q^2}, \quad (13)$$

and

$$B_x(x, Q^2) = \frac{\partial \ln F_2(x, Q^2)}{\partial \ln(1/x)}. \quad (14)$$

For numerical calculations of the slopes we used the following expressions (see [31]):

$$B_Q(x, Q^2) = \frac{Q^2}{2\Delta Q^2} [F_2(x, Q^2 + \Delta Q^2) - F_2(x, Q^2 - \Delta Q^2)], \quad (15)$$

$$B_x(x, Q^2) = -\frac{x}{2\Delta x} \times \frac{F_2(x + \Delta x, Q^2) - F_2(x - \Delta x, Q^2)}{F_2(x, Q^2)}. \quad (16)$$

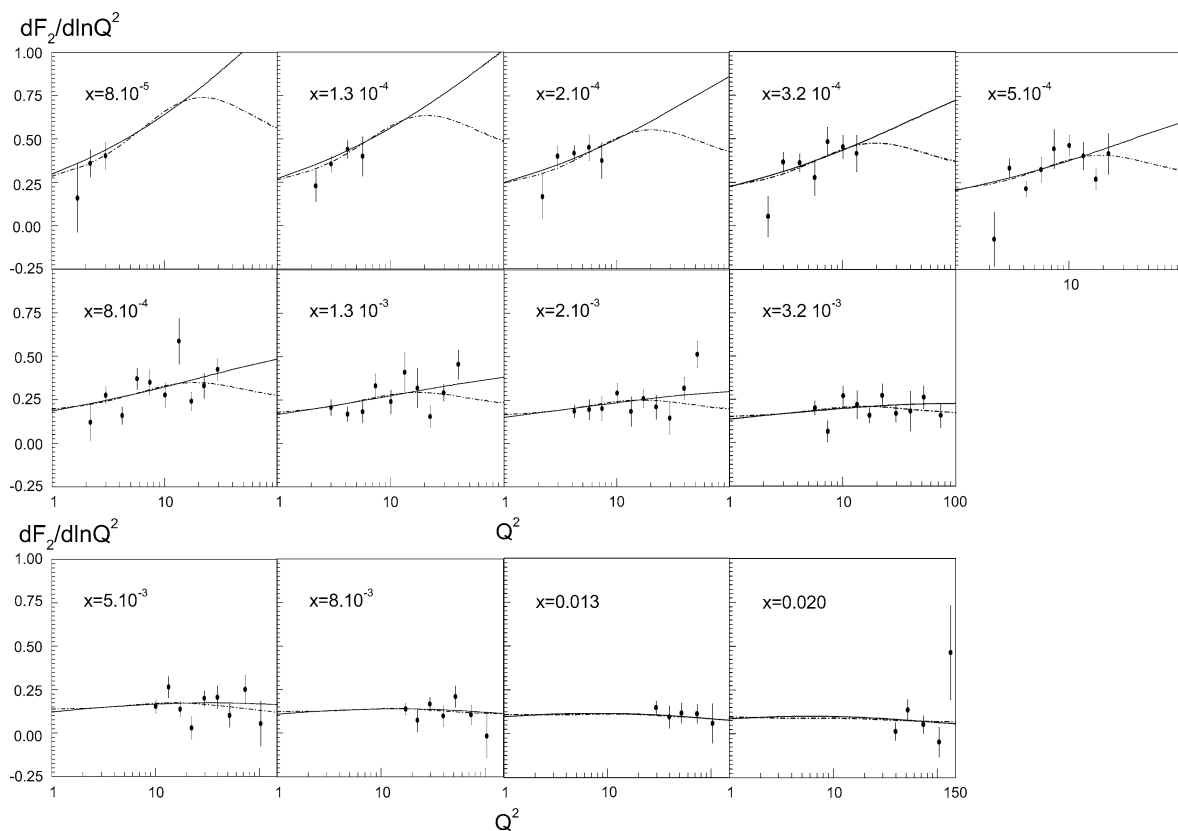


Fig. 5. The result for the  $B_Q$  slope plotted as a function of  $Q^2$  (in  $\text{GeV}^2$ ) for fixed  $x$  compared with the latest H1 data [19]. Same notation of the previous plots.

The early indirect measurements of the slopes contained the shortcoming of correlated bins in the  $(x, Q^2)$  plane [34]. The most recent determinations have a better statistics and the kinematical variables are no longer correlated [19]. Therefore, instead of using the previous two types of slopes [34], which are determined referring two variables, and where one is being averaged (one of them is bounded by a kinematical constraint), we calculated the following four types:

$$B_x(x, Q_{\text{fix}}^2), \quad B_Q(x, Q_{\text{fix}}^2), \\ B_x(x_{\text{fix}}, Q^2), \quad B_Q(x_{\text{fix}}, Q^2).$$

Below, we discuss the results for each slope. In Fig. 4 is shown the slope  $B_Q(x, Q_{\text{fix}}^2)$  in virtualities ranging from  $2 \leq Q^2 \leq 100 \text{ GeV}^2$ . The calculated slopes are in agreement with data, describing well the  $x$ -dependence. Moreover, the results using the CKMT-

type background lie slightly above the logarithmic-type at all kinematical interval. At larger  $Q^2$  the difference between them is more evident, however, in such a region there are no available data to provide a discrimination.

In Fig. 5 are shown the results for the  $B_Q(x_{\text{fix}}, Q^2)$  for Bjorken variable ranging from  $8 \times 10^{-5} \leq x \leq 0.02$ . In the regions where data exist both backgrounds hold. The CKMT-type background select parameters such that the description is similar to the results using a QCD fit (H1) [19]. The logarithmic-type one presents a typical feature: there is a turn-over (a bump) in virtuality  $Q^2 \approx 15 \text{ GeV}^2$ , in a similar way as the Regge dipole pomeron [21]. Both coincide starting at  $x = 3.2 \times 10^{-3}$ .

In Fig. 6 are shown the results for the  $B_x(x_{\text{fix}}, Q^2)$  for Bjorken variable ranging from  $7 \times 10^{-5} \leq x \leq 0.019$ . Such a quantity corroborates a phenomenological pomeron having  $Q^2$ -dependent intercept. For this

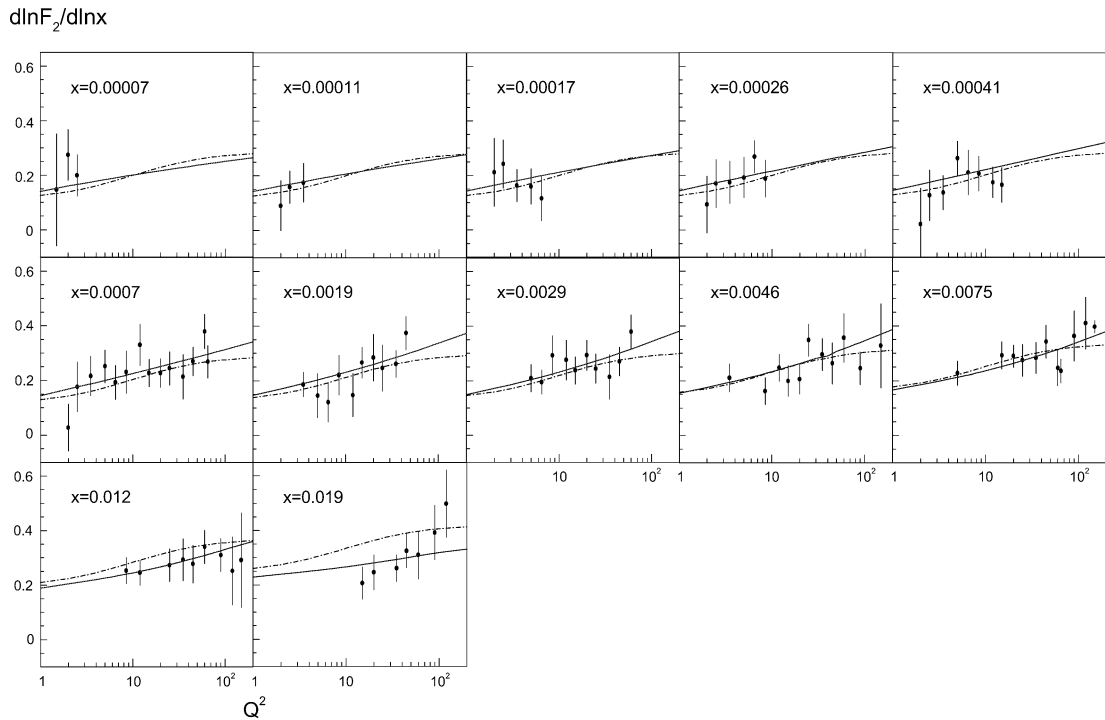


Fig. 6. The result for the partial derivative  $B_x$  slope plotted as a function of  $Q^2$  for fixed  $x$  compared with the latest H1 data [20]. Same notation of the previous plots.

slope, practically the same result is obtained considering the two models for the background. A significative deviation is verified only at larger  $x \sim 0.012$ .

In Fig. 7 are shown the slope  $B_x(x, Q_{\text{fix}}^2)$  for virtualities ranging from  $1.5 \leq Q^2 \leq 150 \text{ GeV}^2$ . One verifies that the slope is independent of Bjorken  $x$  for  $x \leq 0.01$ , in agreement with the experimental measurements and consistent with the H1 NLO QCD fit [20]. The two backgrounds deviate from each one in the transition region  $\approx 0.01$ , suggesting that the large- $x$  region would be described differently taking distinct backgrounds. In a rough extrapolation, the CKMT-type seems to be favoured, whereas the logarithmic-type would overestimate the large  $x$  slope values.

## 5. Conclusions

When looking in the region of high energy limit, we are faced with the lack of connection between the Regge approach and perturbative QCD in describing the asymptotic behavior of the hadronic (and photon-

initiated) cross sections. The main issue is whether perturbation theory may shed light on the origin and the nature of such physics, i.e., the pomeron-induced reactions. In this work we have studied in detail the application of the finite sum of gluon ladders, associated with a truncated BFKL series, for the inclusive structure function considering up to the two rung ladder contribution. This provides the asymptotic behavior expected from the Froissart bound. The truncated series describes a broad region on  $Q^2$ , however, with a formally large  $\chi^2/\text{dof}$  due to the limited number of adjustable parameters. A large span in  $Q^2$  is obtained if we consider a non-perturbative background, modeled here as a soft pomeron. The resulting picture is very close to the two-pomeron model of Donnachie–Landshoff, with the hard pomeron settled by the finite sum of ladders. As a result, the structure function is described with good confidence level for data lying at  $x \leq 0.025$  and  $0.045 \leq Q^2 \leq 1500 \text{ GeV}^2$ . The description of data with  $x \geq 0.025$  is expected to hold, since we have introduced the threshold factor,  $(1-x)^7$ . There is no unambiguous sensitivity to

$d\ln F_2/d\ln x$

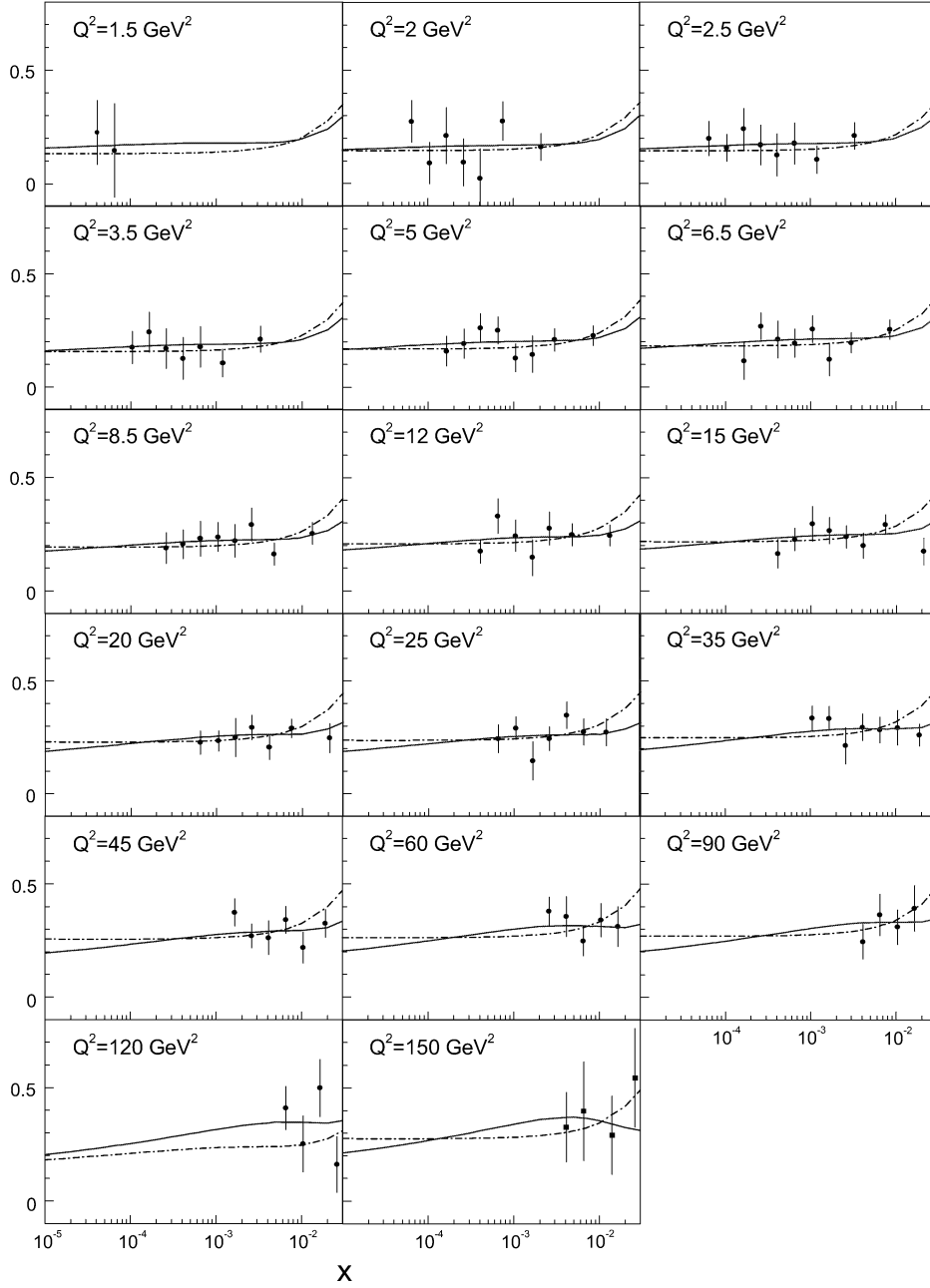


Fig. 7. The result for the  $B_x$  slope plotted as a function of  $x$  for fixed  $Q^2$  virtualities compared with the latest H1 data [20]. Same notation of the previous plots.

the specific choice of the background, although the CKMT-type is preferred due to the reduced number of additional parameters. The region where the deviation between the backgrounds is more important stays in the very low virtualities ( $Q^2 \leq 1 \text{ GeV}^2$ ), with the logarithmic-type providing a better  $\chi^2/\text{dof}$ .

Using the mentioned result, the updated slopes of the proton structure function can be numerically calculated considering the two backgrounds. In general grounds, both choices for the non-perturbative piece seem to be in agreement with the available data, with deviations in kinematical regions where there are not measurements to clarify the analysis. For example, the CKMT-type provides a description closer to the NLO QCD fits, favoured due to the reduced number of additional constants. For instance, it selects parameters leading to the growth with  $Q^2$  at small  $x$  for the slope  $(\partial F_2/\partial \ln Q^2)_x$ , and the flat behavior on small Bjorken  $x$  at fixed  $Q^2$  for the slope  $(\partial \ln F_2/\partial \ln x)_{Q^2}$ , with similar features as in the QCD fits.

## Acknowledgements

M.V.T.M. thanks Prof. Peter Landshoff for useful enlightenings on the two-pomeron model. This work was partially supported by CNPq, Brazil.

## References

- [1] Yu.L. Dokshitzer, Sov. Phys. JETP 46 (1977) 641; G. Altarelli, G. Parisi, Nucl. Phys. B 126 (1977) 298; V.N. Gribov, L.N. Lipatov, Sov. J. Nucl. Phys. 28 (1978) 822.
- [2] M. Klein, Status Report on THERA Studies, in: Proceedings of the DIS2000 Conference, Liverpool, 2000.
- [3] A.H. Mueller, Phys. Lett. B 396 (1997) 251.
- [4] M. Klein, Int. J. Mod. Phys. A 15S1 (2000) 467.
- [5] L.V. Gribov, E.M. Levin, M.G. Ryskin, Nucl. Phys. B 188 (1981) 555; L.V. Gribov, E.M. Levin, M.G. Ryskin, Phys. Rep. 100 (1983) 1; A.L. Ayala, M.B. Gay Ducati, E.M. Levin, Nucl. Phys. B 493 (1997) 305; A.L. Ayala, M.B. Gay Ducati, E.M. Levin, Nucl. Phys. B 511 (1998) 355; Ya. Balitsky, Nucl. Phys. B 463 (1996) 99; Yu. Kovchegov, Phys. Rev. D 60 (1999) 034008.
- [6] K. Golec-Biernat, M. Wüsthoff, Phys. Rev. D 59 (1999) 014017; K. Golec-Biernat, M. Wüsthoff, Phys. Rev. D 60 (1999) 114023; E. Gotsman et al., Phys. Lett. B 492 (2000) 47; E. Gotsman et al., Nucl. Phys. A 683 (2001) 383; E. Gotsman et al., Phys. Lett. B 506 (2001) 289; M.B. Gay Ducati, M.V.T. Machado, hep-ph/0111093.
- [7] E.A. Kuraev, L.N. Lipatov, V.S. Fadin, Phys. Lett. B 60 (1975) 50; E.A. Kuraev, L.N. Lipatov, V.S. Fadin, Sov. Phys. JETP 44 (1976) 443; E.A. Kuraev, L.N. Lipatov, V.S. Fadin, Sov. Phys. JETP 45 (1977) 199; Ya. Balitsky, L.N. Lipatov, Sov. J. Nucl. Phys. 28 (1978) 822.
- [8] M. Froissart, Phys. Rev. 123 (1961) 1053; A. Martin, Phys. Rev. 129 (1963) 1462.
- [9] G.P. Salam, Acta Phys. Pol. B 30 (1999) 3679, and references therein.
- [10] Yu. Kovchegov, Phys. Rev. D 61 (2000) 074018; K. Golec-Biernat, L. Motyka, A.M. Stasto, hep-ph/0110325.
- [11] M.B. Gay Ducati, M.V.T. Machado, Phys. Rev. D 63 (2001) 094018; M.B. Gay Ducati, M.V.T. Machado, Nucl. Phys. (Proc. Suppl.) B 99 (2001) 265.
- [12] M.B. Gay Ducati, M.V.T. Machado, hep-ph/0104192.
- [13] R. Fiore et al., Phys. Rev. D 63 (2001) 056010.
- [14] N. Armesto, J. Bartels, M.A. Braun, Phys. Lett. B 442 (1998) 459.
- [15] M. Ciafaloni, D. Colferai, Nucl. Phys. B 538 (1999) 187; M. Ciafaloni, D. Colferai, G.P. Salam, JHEP 9910 (1999) 017; M. Ciafaloni, D. Colferai, Phys. Lett. B 452 (1999) 372; M. Ciafaloni, D. Colferai, G.P. Salam, Phys. Rev. D 60 (1999) 114036.
- [16] J. Kwiecinski, L. Motyka, Phys. Lett. B 438 (1998) 203; J. Kwiecinski, L. Motyka, Phys. Lett. B 462 (1999) 203; J. Kwiecinski, L. Motyka, Eur. Phys. J. C 18 (2000) 343.
- [17] K. Kontros, A. Lengyel, Z. Tarics, hep-ph/0011398.
- [18] J.R. Forshaw, M.G. Ryskin, Z. Phys. C 68 (1995) 137.
- [19] H1 Collaboration, C. Adloff et al., Eur. Phys. J. C 21 (2001) 33.
- [20] H1 Collaboration, C. Adloff et al., Phys. Lett. B 520 (2001) 183.
- [21] P. Desgrolard, A. Lengyel, E. Martynov, JHEP 0202 (2002) 029, hep-ph/0110149.
- [22] J.R. Forshaw, D.A. Ross, QCD and the Pomeron, Cambridge Univ. Press, 1997.
- [23] Ya. Balitsky, E. Kuchina, Phys. Rev. D 62 (2000) 074004.
- [24] P. Desgrolard, A. Lengyel, E. Martynov, Eur. Phys. J. C 7 (1999) 655; P. Desgrolard, L. Jenkovszky, F. Paccanoni, Eur. Phys. J. C 7 (1999) 263.
- [25] H. Navelet, R. Peschanski, Ch. Royon, S. Wallon, Phys. Lett. B 385 (1996) 357.
- [26] M.B. Gay Ducati, V.P. Gonçalves, Phys. Lett. B 437 (1998) 177.
- [27] A. Donnachie, P.V. Landshoff, Phys. Lett. B 518 (2001) 63, and references therein.
- [28] J.R. Cudell, G. Soyez, Phys. Lett. B 516 (2001) 77.



- [29] P. Desgrolard, E. Martynov, *Eur. Phys. J. C* 22 (2001) 479.
- [30] A. Capella, A.B. Kaidalov, C. Merino, J. Tran Thanh Van, *Phys. Lett. B* 337 (1994) 358.
- [31] A.B. Kaidalov, C. Merino, D. Pertermann, *Eur. Phys. J. C* 20 (2001) 301.
- [32] ZEUS Collaboration, M. Derrick et al., *Zeit. Phys. C* 72 (1996) 399.
- [33] ZEUS Collaboration, J. Breitweg et al., *Phys. Lett. B* 407 (1997) 432.
- [34] ZEUS Collaboration, J. Breitweg et al., *Eur. Phys. J. C* 7 (1999) 609.
- [35] ZEUS Collaboration, J. Breitweg et al., *Nucl. Phys. B* 487 (2000) 53.
- [36] ZEUS Collaboration, S. Chekanov et al., *Eur. Phys. J. C* 21 (2001) 443.
- [37] H1 Collaboration, T. Ahmed et al., *Nucl. Phys. B* 439 (1995) 471.
- [38] H1 Collaboration, S. Aid et al., *Nucl. Phys. B* 470 (1996) 3.
- [39] H1 Collaboration, C. Adloff et al., *Nucl. Phys. B* 497 (1997) 3.
- [40] H1 Collaboration, C. Adloff et al., *Eur. Phys. J. C* 13 (2000) 609.